

Chapter 2

Fluorescence-Based Methods for the Study of Protein Localization, Interaction, and Dynamics in Filamentous Fungi

Oier Etxebeste and Norio Takeshita

2.1 Introduction

Many filamentous fungal species are directly relevant to humans and human activities (Jiang et al. 2013). Many play important roles in industry, agriculture, and medicine (Gibbs et al. 2000). For example, antibiotics or immunosuppressants such as penicillins, griseofulvin, cephalosporin, and cyclosporins are obtained from *Penicillium*, *Chepalosporium*, *Tolepocladium*, and *Cylindrocarpon* species, respectively (Gutierrez-Correa et al. 2012; Kürnsteiner et al. 2002). Mycotoxins such as ochratoxins, aflatoxins, and zearalenone are produced by *Aspergillus*, *Penicillium*, and *Fusarium* species, while enzymes such as glucose oxidase, pectinase, xylanase, or glycoamylases are commercially produced from *Aspergilli* (Gibbs et al. 2000). Other filamentous fungal species are pathogens of plants and animals, including humans (Jiang et al. 2013). Commonly carried dimorphic (yeast/mold) fungi such as *Candida albicans* or *Candida dubliniensis* and the opportunistic fungus *Aspergillus fumigatus* are the best-known examples of human and animal pathogens that afflict individuals whose immune systems are compromised or dysfunctional (Brand 2012). An unprecedented number of fungal diseases have recently caused some of

N. Takeshita (✉)

Department of Microbiology, Karlsruhe Institute of Technology, Hertzstrasse 16, Geb. 06.40,
76187 Karlsruhe, Baden-Württemberg, Germany
e-mail: norio.takeshita@kit.edu; takeshita.norio.gf@u.tsukuba.ac.jp

Faculty of Life and Environmental Sciences, University of Tsukuba, 1-1-1 Tennoudai Tsukuba,
Tsukuba-shi, Ibaraki 305-8572, Japan

O. Etxebeste

Biochemistry II Laboratory; Applied Chemistry; Faculty of Chemistry. The University of
The Basque Country, Manuel de Lardizabal 3, 20018 San Sebastian, Gipuzkoa, Spain
e-mail: oier.echeveste@ehu.es

© Springer International Publishing Switzerland 2015

T. E. S. Dahms and K. J. Czymmek (eds.), *Advanced Microscopy in Mycology*,
Fungal Biology, DOI 10.1007/978-3-319-22437-4_2

the most severe extinctions in wild species ever witnessed and constantly threaten food security (Fisher et al. 2012). The ProMED website (program for monitoring emerging diseases; www.promedmail.org) documented, over the period from 1995 to 2010, an increase from 0.4 to 5.4% in the relative proportion of plant fungal pathogen alerts (Fisher et al. 2012). *Fusarium graminearum*, *Botrytis cinerea*, and *Ustilago maydis* are three examples of the many filamentous fungal plant pathogens infecting wheat, barley, maize or other plant species (Raffaele and Kamoun 2012; Soanes et al. 2008).

One of the main characteristics enabling filamentous fungi to colonize multiple substrates is their unique growth and developmental behavior as well as their ability to rapidly and efficiently adapt to changing environments. For these reasons, several filamentous fungal species serve as model organisms for understanding basic biological processes. The filamentous ascomycete *Aspergillus nidulans* has been employed worldwide for more than 60 years as a model organism because it is closely related to clinically and economically important *Aspergilli* and it is easily manipulated in the laboratory. A vast array of signaling cascades transduces environmental signals in *A. nidulans* and these pathways control the factors that regulate different morphogenetic programs (see, e.g., Etxebeste et al. 2010). The most characteristic cell type of filamentous fungi is the vegetative hypha. This non-specialized, syncytial (multinucleated) cell is characterized by a continuous polarized (apical) growth mode, mediated at the tip through the addition of new material that is transported from distal regions (Fischer et al. 2008; Harris 2006; Momany 2002; Riquelme 2013; Takeshita et al. 2014). The exposition of *A. nidulans* hyphae to air and light induces the production of conidiophores, asexual reproductive structures bearing thousands of propagules called conidia, which are characterized by low water content and arrested metabolism (Adams et al. 1998; Kües and Fischer 2006). These features permit dispersal and survival under adverse environmental conditions (Gregory 1966). The asexual cycle in *A. nidulans* is normally followed by the production of sexual reproductive structures or cleistothecia, which contain meiospores called ascospores (Pontecorvo et al. 1953; Todd et al. 2007).

The implementation of fluorescence microscopy 20 years ago for the study of filamentous fungi has significantly improved our knowledge of the morphogenetic processes described above. Initial studies followed the subcellular distribution of specific organelles and structures using fluorescent dyes (see, e.g., Fischer and Timberlake 1995; Harris et al. 1994; Momany and Hamer 1997). In 2004, different laboratories standardized the labeling of proteins from *A. nidulans* with fluorescent tags. This was achieved through fusion-polymerase chain reaction (PCR), double-joint PCR (Yang et al. 2004; Yu et al. 2004), or using the GATEWAY cloning systems (Toews et al. 2004), and opened an avenue for *in vivo* systematic analyses of the localization and function of *A. nidulans* proteins. A new generation of fluorescence microscopy techniques have been developed in recent years. A variety of advanced methods (bimolecular fluorescence complementation (BiFC), Förster resonance energy transfer (FRET), fluorescence recovery after photobleaching (FRAP), fluorescence lifetime imaging microscopy (FLIM), photoactivated localization microscopy (PALM), stochastic optical reconstruction microscopy (STORM), etc.) are now available for deeper and more accurate analyses of protein localization,

interaction, dynamics, and degradation (Day and Davidson 2009). Some of these techniques have been successfully implemented in filamentous fungi and will be described here. Focusing mainly on *A. nidulans*, this chapter will provide the reader with an overview of advanced microscopy tools. On the one hand, tools for the analysis of protein interaction will be presented, such as BiFC, FRET, and FLIM. On the other hand, microscopy tools for the study of protein dynamics, time-lapse or stream acquisitions, FRAP, and PALM (Chap. 3) will be discussed.

2.2 Localizing Proteins and Their Interactions

The functionality of a protein is dependent on its correct folding and transport to the corresponding subcellular compartment and, additionally, on its interaction with specific partners or auxiliary proteins. Furthermore, some factors or protein complexes transduce signals from one cell compartment to the nucleus to activate appropriate response mechanisms. This section will focus on the advanced microscopy methods currently available for *in vivo* monitoring of protein interactions within filamentous fungal cells.

2.2.1 Bimolecular Fluorescence Complementation (BiFC)

The analysis of protein interactions in living cells (what, when, and where) is significant because protein interactions offer fundamental mechanisms for specific biological sensing, signaling, and regulation. BiFC analysis is a technology typically used to obtain spatial information about protein interactions, enabling their direct visualization in living cells. It is based on the association of two nonfluorescent fragments of a fluorescent protein that are attached to different components of the same molecular complex. Proteins that are postulated to interact are fused to unfolded complementary fragments of a fluorescent reporter protein and expressed in live cells. Interaction between the two target proteins will bring the fragments of the fluorescent protein within proximity, allowing the formation of the native three-dimensional structure of the reporter protein and emission of its characteristic fluorescent signal (Fig. 2.1a; Kerppola 2006). The BiFC assay has allowed the visualization of numerous protein interactions in many different cell types and organisms (Kodama and Hu 2012).

One example of BiFC analysis in *A. nidulans* is the study of interactions between “cell-end markers” (Higashitsuji et al. 2009; Takeshita et al. 2008). The cell-end markers TeaA and TeaR localize at the tip of hyphae and control growth direction (Fischer et al. 2008). TeaA is transported to the hyphal tip by growing microtubules (MT) and it is anchored at the apical membrane by the interaction with the membrane-associated receptor TeaR (Fig. 2.1b). The N-terminal half of YFP (YFP^N) and the C-terminal half of YFP (YFP^C) were fused to the cell-end markers. YFP fluorescence was not detected for strains expressing either YFP^N–TeaR or

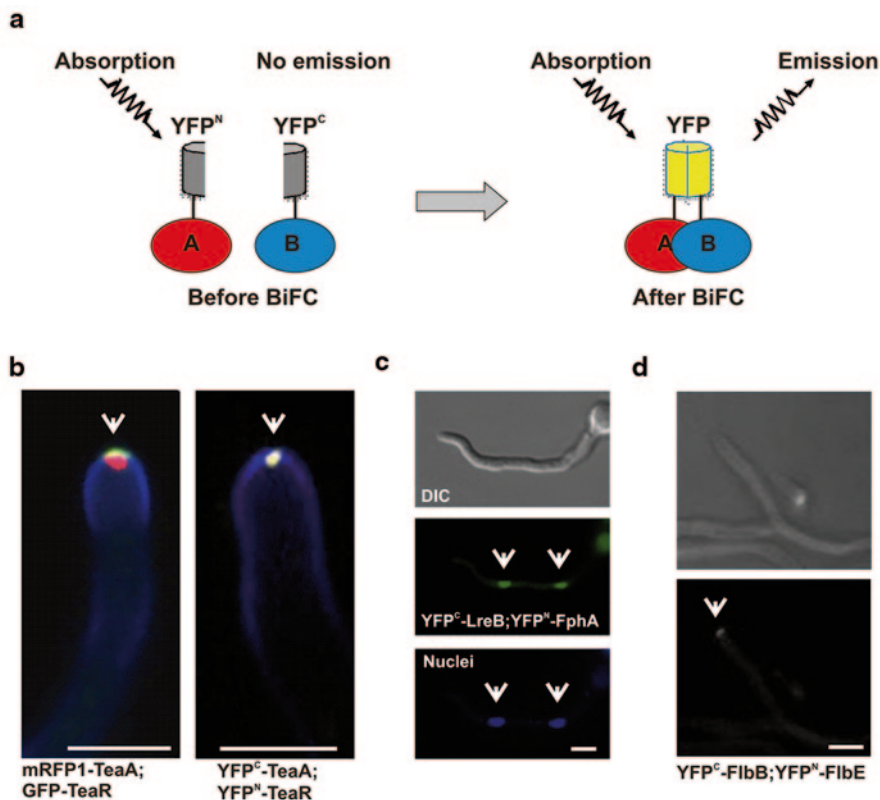


Fig. 2.1 Bimolecular fluorescence complementation (*BiFC*). **a** Schematic representation describing the basis of the technique. Protein A is labeled with the N-terminal half of YFP while Protein B is labeled with the C-terminal half. Formation of a Protein A/Protein B complex brings the YFP fragments within proximity, allowing YFP to acquire its native three-dimensional structure and emit a yellow fluorescence signal. **b**, **c**, and **d** Examples of protein interactions highlighted with the BiFC technique. The interaction between the cell-end markers TeaA and TeaR is shown in panel **b**, that between light receptors LreB and FphA in panel **c**, and the complex formed by the developmental regulators FlbB and FlbE in panel **d**. Scale bar in all panels = 5 μm

YFP^C-TeaA, but was for the strain expressing both YFP^N-TeaR and YFP^C-TeaA as a single point along the apex (Fig. 2.1b), indicating the site of TeaA and TeaR interaction. Another example of BiFC analysis in *A. nidulans* is the study of interactions between blue (LreB) and red (FphA)-light sensors (Purschwitz et al. 2008), key players in the control of fungal development (Bayram et al. 2010; Rodríguez-Romero et al. 2010). While the interaction was first shown by co-immunoprecipitation, BiFC analysis revealed that their interaction took place in nuclei (Fig. 2.1c).

The BiFC technique has also been shown to be a valuable tool for the study of the interaction between apically located regulators of fungal development. The transcription factor FlbB interacts with the small filamentous fungal-specific protein FlbE (Garzia et al. 2010) at the tip of vegetative hyphae (Fig. 2.1d; Garzia et al.

2009). The apical localization of both proteins, which depends on this interaction, is essential to induce conidiophore development (asexual reproduction).

BiFC presents two main drawbacks. On the one hand, false positives can occur when noninteracting proteins are present at high concentrations. On the other hand, BiFC is generally not suitable for following dynamic interactions, since the reconstitution of the fluorescent protein is not completely reversible. However, BiFC has been used to study MT polymerase AlpA, which moves along with the MT plus-end towards the hyphal tip. The cell-end marker TeaA is involved in MT guidance to the polarity site through interaction with AlpA. In a strain expressing both YFP^N-TeaA and YFP^C-AlpA, YFP signals were clearly detected at all hyphal tips (Takeshita et al. 2013). Because AlpA localizes at MT plus-ends, and TeaA accumulates at the hyphal tip cortex, the YFP signal at hyphal tips possibly represents a connection between MT plus-ends and the hyphal tip membrane, suggesting that there is at least a temporary interaction. Although AlpA does not localize at hyphal tips permanently due to MT depolymerization, the YFP signal was nonetheless stable. Tracing interaction dynamics, however, requires other methods such as FRET.

2.2.2 Förster Resonance Energy Transfer (FRET)

In living cells, protein interactions play a key role in regulating many signal transduction pathways. FRET is a method that can be used to track dynamic interactions based on energy transfer between two chromophores. A donor chromophore (cyan fluorescent protein (CFP) in Fig. 2.2a), initially in its excited electronic state, may transfer energy to an acceptor chromophore (yellow fluorescent protein (YFP) in Fig. 2.2a) through nonradiative dipole–dipole coupling. The efficiency of this energy transfer is inversely proportional to the sixth power of the distance between the donor and the acceptor, making FRET extremely sensitive to small distances (Tsien 1998). Measurements of FRET efficiency can be used to determine if two fluorophores are within a certain distance of each other, finding wide application in biology and chemistry (Sekar and Periasamy 2003).

One example of a FRET system in filamentous fungi is the dynamic visualization of calcium concentration using the “cameleon” biosensor (Kim et al. 2012). Cameleon consists of calmodulin (CaM) and the CaM-binding module M13 sandwiched between cyan (FRET donor) and yellow (acceptor) fluorescent proteins (Fig. 2.2b; Nagai et al. 2004). In the absence of Ca²⁺, the excitation of CFP leads to the emission of cyan fluorescence. However, when the CaM module is Ca²⁺ loaded, it interacts with M13 and there is a conformational change that brings CFP within FRET distance of YFP, resulting in yellow fluorescence. This reversible interaction is detected as an increase of the YFP to CFP emission ratio.

Monitoring Ca²⁺ by the cameleon system has been performed in diverse living cells (Allen et al. 1999; Rogers et al. 2007). The use of cameleon in *Magnaporthe oryzae*, *Fusarium oxysporum*, and *F. graminearum* showed a cytoplasmic Ca²⁺ change in a pulsatile manner, with no discernible gradient between pulses (Kim et al. 2012), which was age and development dependent. Although the number

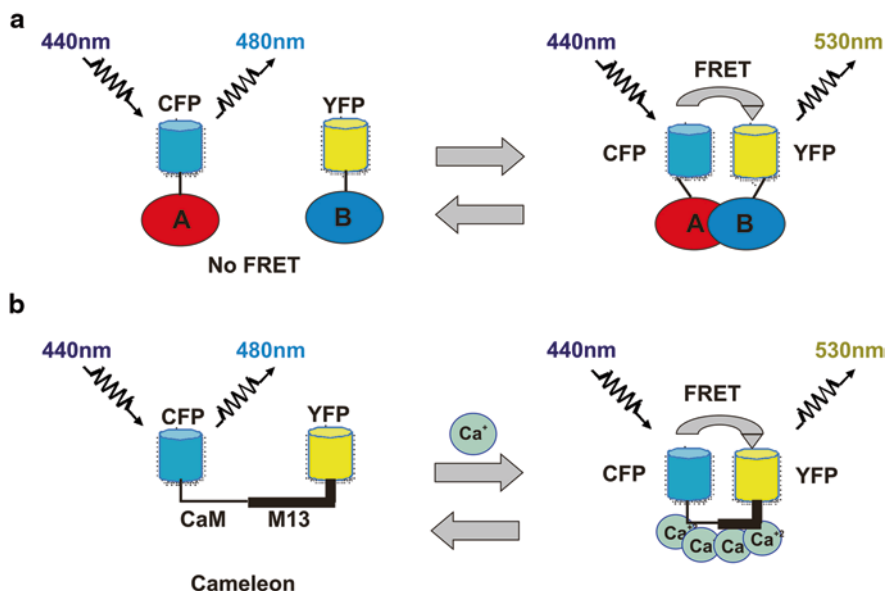


Fig. 2.2 Förster resonance energy transfer (FRET). **a** Schematic representation describing the FRET process between CFP- or YFP-tagged A and B proteins. If Protein A and Protein B do not interact, excitation at 440 nm by CFP leads to emission in cyan (480 nm). The fluorescence of the A protein could be followed in this channel. When Protein A and Protein B form a complex, excitation of Protein A with a 440-nm light is followed by an energy transfer (FRET) from CFP to YFP, which leads to a 530-nm yellow emission. **b** Schematic representation describing the background on the cameleon calcium biosensor. Cameleon consists of calmodulin (*CaM*) and the CaM-binding module M13 sandwiched between cyan (FRET donor) and yellow (acceptor) fluorescent proteins. In the absence of Ca^{2+} , excitation of CFP with a 440-nm light leads to the emission of cyan fluorescence. When the CaM module binds four Ca^{2+} ions and interacts with M13, a conformational change of CFP brings FRET to YFP, leading to the emission of yellow fluorescence. The interaction is reversible, thus allowing researchers to monitor Ca^{2+} concentration changes in living cells

of examples of FRET analysis in filamentous fungi is limited, FRET-based probes have the potential for growing impact in the fungal field, based on successful assays performed in other organisms to detect proteolytic activities, posttranslational modifications, enzymatic activities, Zn^{2+} or cyclic guanosine monophosphate (cGMP) (see references within Ibraheem and Campbell 2010).

2.2.3 Fluorescence Lifetime Imaging Microscopy (FLIM) and FLIM-FRET

FLIM bases contrast on the lifetime of individual fluorophores, rather than their emission spectra, producing an image based on the differences in the excited state decay rates. The fluorescence lifetime is defined as the average time that a molecule remains in an excited state prior to returning to the ground state by emitting

a photon. As the fluorescence lifetime does not depend on concentration, absorption by the sample, sample thickness, photobleaching, and/or excitation intensity, FLIM is more convenient for quantification than intensity-based methods (Chang et al. 2007). It can also be applied to tracking signaling events inside living cells, such as monitoring changes in intracellular ions and detecting protein–protein interactions.

The principle behind FLIM–FRET relies on the fact that FRET is a very efficient fluorescence quencher and in the presence of a suitable acceptor the lifetime of the donor will decrease. Since the fluorescence decay of a donor/acceptor population contains the fluorescence of quenched and nonquenched molecules, quantitative FLIM–FRET measurements thus require the average lifetime of the donor with and without quenching so that FRET efficiency can be calculated based on the ratio thereof. FLIM–FRET analysis has been applied to the study of v-SNARE/t-SNARE interactions in *Trichoderma reesei* (Altenbach et al. 2009; Valkonen et al. 2007). The high spatial resolution imaging in living cells showed that the site of ternary SNARE complex formation is spatially segregated at distinct sites of the apical plasma membrane.

2.3 Protein Localization and Dynamics

This section will introduce advanced microscopy techniques, some of which are covered in depth in other chapters of this volume, that facilitate the analysis of protein transport and localization within the context of the cell cycle or the growth phase. Standardized fluorescent protein labeling methods for filamentous fungal proteins (Toews et al. 2004; Yang et al. 2004; Yu et al. 2004) in conjunction with fluorescence or confocal microscopy (see Chap. 1) have enabled *in vivo* analyses of protein dynamics. This has been achieved mainly through time-lapse acquisitions over short- or long-time intervals, respectively, and superimposing or viewing the images as movies (see references below). Time-lapse fluorescence analysis of the proteins forming the nuclear pore complex (NPC), the multimeric channel that guides the transport of macromolecules between the nucleus and the cytoplasm (De Souza and Osmani 2007; Fiserova and Goldberg 2010) in *A. nidulans* showed that structural changes in the pore structure depend on the progression of the cell cycle (Osmani et al. 2006). Similarly, Markina-Iñarrairaegui and coworkers (Markina-Iñarrairaegui et al. 2011) systematically analyzed the variable localization pattern of nuclear transporters, molecules involved in the translocation of cargoes through NPCs (Espeso and Osmani 2008), during the *A. nidulans* cell cycle (Fig. 2.3a). By streaming image data, the movement of several filamentous fungal proteins has been tracked. For example, anterograde and retrograde early-endosome (EE) transports between the tip and distal hyphal compartments have been shown in various filamentous fungal species to be facilitated by MTs (Fig. 2.3b; Abenza et al. 2009; Penalva et al. 2012; Steinberg 2012). Kinesin-3 and dynein motor proteins cooperate in this bidirectional transport of EEs (Schuster et al. 2011), which seems to be necessary for the transport of, for example, *A. nidulans* nuclear transporters such as karyopherins KapA and KapB (Etxebeste et al. 2013; Zekert and Fischer 2009).

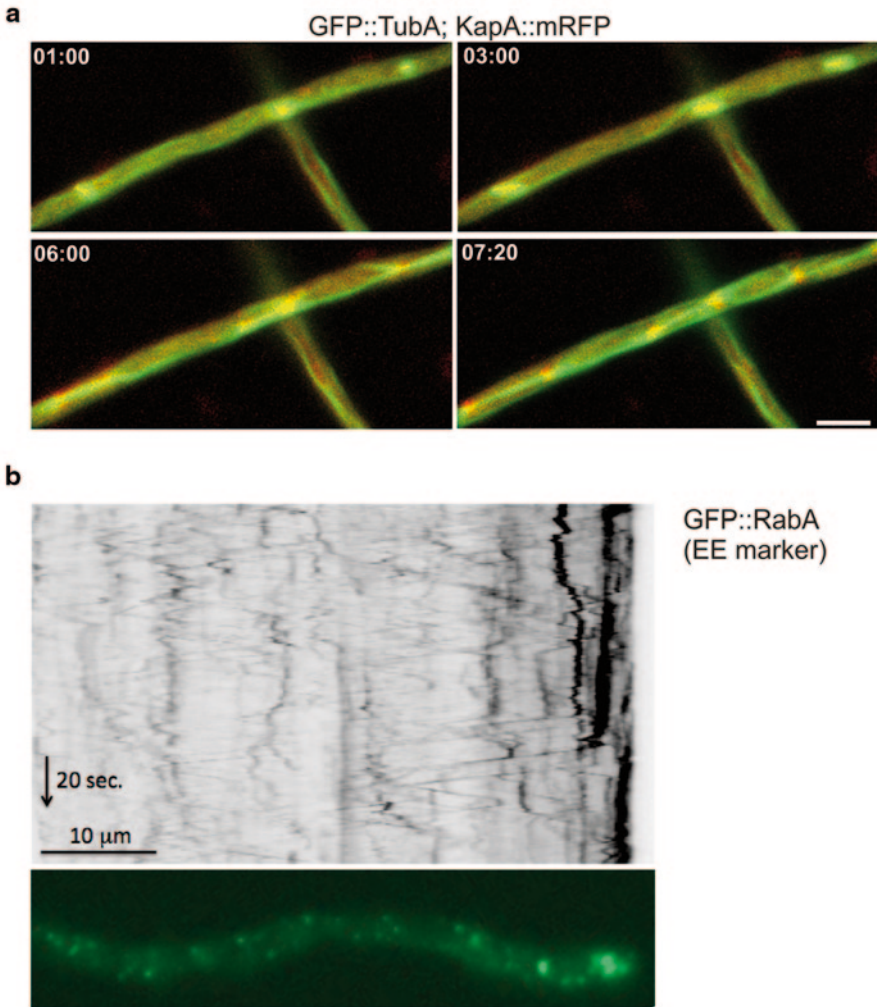


Fig. 2.3 Time-lapse and stream acquisition. **a** Selected frames from a time-lapse series (29 frames, 3 frames of 200 ms per min) showing a vegetative hypha of *Aspergillus nidulans* expressing KapA::mRFP and GFP::TubA chimeras during mitosis. Yellow fluorescence indicates colocalization of both proteins. Time is indicated in min:sec. Both proteins co-localize at the mitotic spindle. Scale bar = 5 μm. **b** Kymograph generated from a 20 s stream acquisition corresponding to a hypha expressing the early endosome marker RabA fused to GFP (Abenza et al. 2009). Scale bar = 10 μm

2.3.1 Fluorescent Recovery After Photobleaching (FRAP)

FRAP is another fluorescence-based microscopy technique which, when combined with time-lapse acquisitions and confocal microscopy (Chap. 1), can provide valuable information about the kinetic properties of a protein (Lippincott-Schwartz et al.

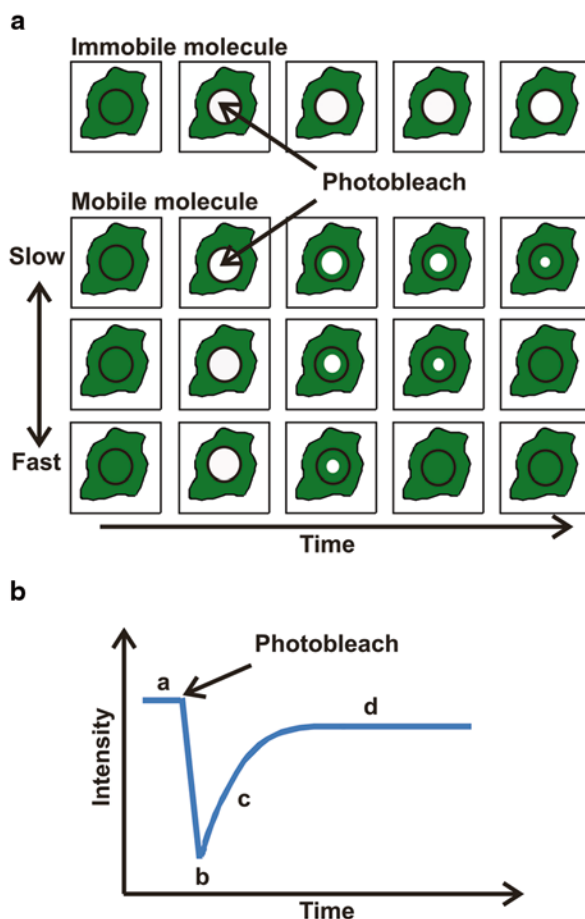


Fig. 2.4 Fluorescence recovery after photobleaching (FRAP). **a** Schematic representation showing the basis of the FRAP technique. Photobleaching of a region of interest (ROI) within the cell analyzed allows the measurement of the fluorescence recovery pace with molecules coming from the surrounding, non-photobleached, area. **b** Baseline of fluorescence (*a*) is reduced after photobleach (*b*). Over time, the fluorescent intensity in the photobleached area increases as unbleached molecules diffuse into this area (*c*). Later, there is a stabilization of the amount of fluorescence recovery (*d*)

2003). Photobleaching of a fluorophore, the extinction of its fluorescence through irradiation with directed high-intensity laser typically of short duration, is usually limited to a selected region (region of interest (ROI)) of the sample being analyzed (Fig. 2.4a; Klonis et al. 2002). After photobleaching, specific populations of fluorescently tagged proteins can be followed over time as they repopulate the ROI (Klonis et al. 2002; Lippincott-Schwartz et al. 2003). The rate of recovery is quantified to determine kinetics of protein movement, which can be fast, slow, or null, and can be mediated through binding/dissociation, diffusion, or transport processes (Fig. 2.4a, b; Lippincott-Schwartz et al. 2003).

Confocal (Chap. 1) FRAP is widely used and has been adapted to study a variety of filamentous fungal species and cellular processes. FRAP has been used to analyze MT dynamics during hyphal growth (Sampson and Heath 2005) or the role of specific myosins, such as MyoE, the myosin V homolog in *A. nidulans* (Taheri-Talesh et al., 2012). In *A. oryzae*, FRAP showed that secretory vesicles were constitutively transported to the septal plasma membrane (Hayakawa et al. 2011; Read 2011). FRAP studies in *Neurospora crassa* analyzed the MT polymerization and dynamics during cell morphogenesis (Mourino-Perez et al. 2006) and the movement and distribution of nuclei (Ramos-Garcia et al. 2009).

FRAP has also served as a valuable tool for the study of filamentous fungal pathogens. For example, Giraldo and coworkers have recently described two secretion systems from *Magnaporthe oryzae* that facilitate plant tissue invasion (Giraldo et al. 2013). In the corn smut pathogen *U. maydis*, FRAP was used to analyze the dynamics of the myosin motor domain-containing chitin synthase Mcs1 (Schuster et al. 2012) and the MT-dependent motility of NPCs (Steinberg et al. 2012).

It should be taken into consideration that high-powered lasers could damage the sample being analyzed and induce artifacts. Furthermore, cell geometry and protein compartmentalization should be carefully studied for the selection of the appropriate model for the measurement of diffusion coefficients.

2.3.2 Photoconvertible Tagging of Filamentous Fungal Proteins

A recently developed array of FPs include photoswitchable (change between fluorescent and dark states), photoactivatable (fluorescence intensity increases upon irradiation), and photoconvertible fluorescent protein (PCFP; change from one emission wavelength to another) tags, whose spectral properties can be directly modified by a pulse of light (Chudakov et al. 2007b; Day and Davidson 2009). Dendra2 is a green-to-red monomeric PCFP which allows unique options for photolabeling and tracking of fusion proteins in living cells (Fig. 2.5a; Chudakov et al. 2007a, b; Gurskaya et al. 2006): (1) the tagged protein can be tracked in green before photoconversion; (2) Dendra2 can be photoactivated using either UV (405 nm) or blue (488 nm) light, and (3) the activated red Dendra2 signal renders high photostability (Chudakov et al. 2007b). Dendra2 has mostly been applied to studying higher eukaryotic cells and yeasts (see, e.g., references within Chudakov et al. 2007b; Jasik et al. 2013; Onischenko et al. 2009), but was recently used for the first time in filamentous fungi (Perez-de-Nanclares-Arregi and Etxebeste 2014).

The method was adapted to tracking low-expression proteins from *A. nidulans*, such as the apical developmental regulator FlbB (see Sect. 2.1; Etxebeste et al. 2009; Garzia et al. 2009; Harris 2009; Perez-de-Nanclares-Arregi and Etxebeste 2014), whose expression was driven through the constitutive *gpdA^{mini}* promoter (Pantazopoulou and Penalva 2009). As expected, green fluorescence was detected at the tip and nuclei before photoconversion, while red fluorescence was undetectable (Fig. 2.5b; Etxebeste et al. 2008; Etxebeste et al. 2009; Garzia et al. 2009).

Advanced Microscopy in Mycology

Dahms, T.E.S.; Czymmek, K.J. (Eds.)

2015, XII, 164 p. 64 illus., 56 illus. in color., Hardcover

ISBN: 978-3-319-22436-7